Path Integral−Molecular Dynamics Study of Electronic States in Supercritical Water

Daniel Laria*,†,‡ and Munir S. Skaf§

Unidad Actividad Química, Comisión Nacional de Energía Atómica, Avenida Libertador 8250, 1429, Buenos Aires, Argentina, Departamento de Química Inorgánica, Analítica y Química-Física e Inquimae, Facultad de Ciencias Exactas y Naturales, Universidad de Buenos Aires Ciudad Universitaria, Pabellón II, 1428, Buenos Aires, Argentina, and Instituto de Química, Universidade Estadual de Campinas, Cx. P. 6154, Campinas, SP 13083-970, Brazil

Received: May 22, 2002

We have carried out path integral−molecular dynamics simulations to describe microscopic details of excess electrons in supercritical water over a wide range of solvent densities, ρ_w, along the $T = 645$ K isotherm. The well-tested simple-point charge model for water was used. The transition from localized to quasifree states described in terms of the electron spatial extent is observed in the vicinity of $\rho_w = 0.15$ g cm^{-3}. For smaller densities, the electron undergoes quantum tunneling through nearest neighboring water molecules. The ground-state absorption spectrum exhibits significant red shifts in the absorption maxima with decreasing density, showing reasonable agreement with recent pulse radiolysis measurements.

I. Introduction

Supercritical states of water provide environments with special properties where many reactive processes with important technological applications take place.[1] Two key aspects combine to make chemical reactivity under these conditions so peculiar: the solvent high compressibility, which allows for large density variations with relatively minor changes in the applied pressure, and the drastic reduction of bulk polarity, clearly manifested in the drop of the macroscopic dielectric constant from $\epsilon \approx 80$ at room temperature to $\epsilon \approx 6$ at near-critical conditions. From a microscopic perspective, the unique features of supercritical fluids as reaction media are associated with density inhomogeneities present in these systems.[2] Over the last twenty five years, a series of pulse radiolysis experiments has provided evidence that electronic states can be supported in aqueous supercritical environments[3−6] and that the spectral characteristics of solvated electrons can be used to investigate the structure of the local inhomogeneities in supercritical systems.[7] This opens interesting questions pertaining the nature of the electronic quantum states under such conditions and, more specifically, about the extent of spatial delocalization of the electron as we move from dense liquid environments down to vaporlike ambients. It is generally believed that a gradual transition from localized states, typical of dense polar fluids, to quasifree electronic states under supercritical conditions leads to the observed red shifts in the optical absorption spectra and to significant changes in the dynamical behavior of the electron, most notably a dramatic increase in its drift mobility.[8,9] One interesting feature of the absorption spectra of nearly supercritical water at $T = 623$ K reported by Jortner and collaborators[3] is the weak density dependence of the spectral shift over a wide interval ranging from 1 down to 0.05 g cm^{-3}. This behavior suggests that the electron localization in aqueous supercritical environments persists at densities as low as 0.05 g cm^{-3}. This feature has also been corroborated by time-of-flight measurements on photoinjected electrons in steam-like environments along the $T = 523$ K isotherm which show a sharp drop of practically 3 orders of magnitude in the electronic mobility at densities near 0.02 g cm^{-3}.[8] Although physically sensible, this picture has not yet been fully verified by simulation approaches that include a detailed microscopic description of the particular polar environment under consideration.[10]

The study of excess electrons in different aqueous environments has received considerable attention from both experimental and theoretical viewpoints. Analytical developments[11] and computer simulations have shed light on microscopic details of a rich variety of electronic behaviors in water at ambient conditions,[12−14] hot water,[10,15] and clusters.[16] In this work we apply combined path integral−molecular dynamics (PIMD) simulation techniques to examine the characteristics of the excess electronic states in different supercritical states of water. Our results show the existence of a well defined transition from spatially localized to delocalized electronic state as the density drops below ∼0.15 g cm^{-3}. For more dilute conditions, quantum tunneling through the nearest neighboring water molecules is also observed. The organization of the present paper is as follows: In section II we provide details about the model and implemented methodology. Results are shown in section III. The main conclusions are presented in section IV.

II. Methods and Model

The systems under investigation consisted of an electron coupled to a classical bath of $N_w = 342$ water molecules. The simulation methodology is based on the well-known isomorphism[17] that exists between the statistical mechanics of the quantum electron path and that of a classical cyclic polymer containing P pseudoparticles ("beads") with harmonic nearest-neighbor interactions. In this representation, the statistically averaged electron probability amplitude can be pictured by the spatial distribution of the polymer beads. To sample configuration space, we implemented a molecular dynamics algorithm that included a reversible multiple time scale integrator of

* Corresponding author. Email:dhlaria@cnea.gov.ar.
† Comisión Nacional de Energía Atómica.
‡ Universidad de Buenos Aires Ciudad Universitaria.
§ Universidade Estadual de Campinas.

10.1021/jp021278b CCC: $22.00
Published on Web 08/13/2002

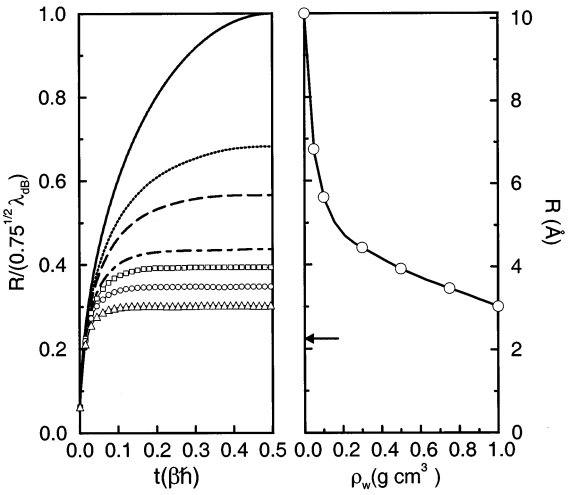

Figure 1. Left: Root-mean-square correlation function for the aqueous electron along the $T = 645$ K isotherm. Lines from top to bottom correspond to $\rho_w = 0.0$ (free electron), 0.05, 0.1, 0.3, 0.5, 0.7, and 1.0 g cm^{-3}, respectively. Right: Correlation length for the electron polymer vs density. The arrow indicates the room-temperature result.

Newton's equations of motion and the staging ansatz.[18] Chains of three Nosé−Hoover thermostats were coupled to each Cartesian coordinate of the electron polymer to provide proper ergodic canonical dynamics. The classical bath is also coupled to an identical thermostat chain. Full details of the method can be found in ref 18. The well-tested SPC model[19] is used to describe water intermolecular interactions. The electron−solvent coupling is given by the pseudopotential of Schnitker and Rossky.[20] The simulations correspond to canonical runs along the $T = 645$ K isotherm, which is 10% above the critical temperature of SPC water, $T_C^{SPC} \approx 587$ K.[21] In choosing this thermal regime, we tried to avoid significant effects arising from criticality of the solvent. Several simulations were performed for solvent densities in the range $0.05 \leq \rho_w \leq 1.0$ g cm^{-3}. The number of polymer beads was set to $P = 1000$, of which 20 are endpoints and the rest corresponds to staging masses.[18] All interactions were smoothly brought to zero at half the simulation boxlength in an interval of 0.5 Å by a fourth-degree spline.

III. Results and Discussion

The most direct route to analyze the extent of the electronic localization is by examining the behavior of the mean square correlation function for the solvated electron-polymer $R^2(t)$ defined by:

$$R^2(t - t') = \langle |\mathbf{r}(t) - \mathbf{r}(t')|^2 \rangle, \qquad 0 \leq t - t' \leq \beta\hbar \qquad (1)$$

where $\mathbf{r}(t)$ represents the electron position at imaginary time t and β^{-1} is Boltzmann constant times the temperature. At low densities ($\rho_w < 0.1$ g cm^{-3}), the correlation functions (Figure 1, left panel) look similar to those corresponding to Gaussian free polymers: Interparticle distances along the electron polymer are characterized by a wide variety of lengthscales, up to roughly half the de Broglie thermal wavelength, $\lambda_{dB}(T = 645\ \text{K}) \approx 12$ Å. As we move toward the density regime of typical dense fluids, there is a qualitative change in the temporal behavior of the curves. After a short transient lasting $\sim 0.1\ \beta\hbar$, the curves level off at practically plateau values. This time independence has been interpreted as a signature of statistical dominance of the ground state on the behavior of the electron.[22] Expressed in terms of the spectrum of instantaneous electron eigenvalues, this situation corresponds to large energy gaps ($\gg k_B T$) between the ground and the manifold of excited states. More direct evidence of this transition is acquired by inspecting the density dependence of the correlation length for the electron polymer $R = R(\beta\hbar/2)$, shown in the right panel of Figure 1. The sudden drop to practically half of the ideal, noninteracting, $\rho_w = 0$ value within a narrow density interval and an abrupt change in the slope of the curve reveals the onset of the electronic localization at $\rho_w \approx 0.15$ g cm^{-3}.

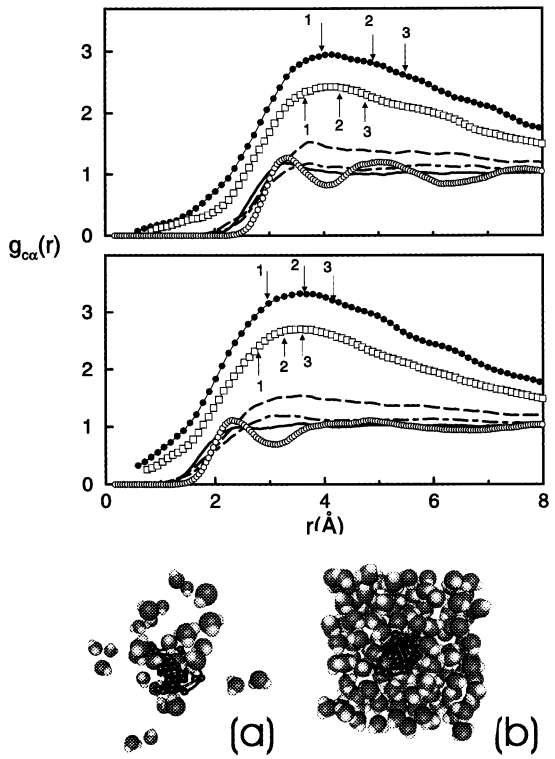

Figure 2. Top and middle panels: Electron centroid−water pair correlation functions for different supercritical states along the $T = 645$ K isotherm. Top, $g_{cO}(r)$, middle, $g_{cH}(r)$. $\rho_w = 0.05$, 0.1, 0.3, 0.5, and 1.0 g cm^{-3} are depicted by solid circles, open squares, dashed lines, dot−dashed lines, and solid lines, respectively. The arrows indicate the coordination numbers at selected distances. Also shown are the results for ambient water (open circles). Bottom panel: Snapshots of molecular configurations for the solvated electron polymer at two supercritical densities. (a) $\rho_w = 0.05$ g cm^{-3}; (b) $\rho_w = 1$ g cm^{-3}.

The analysis of different electron−solvent centroid spatial correlations provides complementary information about the characteristics of the spatial deconfinement as the density lowers. The electron centroid is defined as $\mathbf{r}_c = \int_0^{\beta\hbar}[\mathbf{r}(t)\, dt]/(\beta\hbar)$. In Figure 2 we present results for different solvent−centroid pair correlation function $g_{c\alpha}(r)$, (α = O, H):

$$g_{c\alpha}(r) = \frac{1}{4\pi r^2 \rho_\alpha} \left\langle \sum_i \delta(|\mathbf{r}_c - \mathbf{R}_i^\alpha| - r) \right\rangle \qquad (2)$$

where $\mathbf{R}_i^\alpha$ denotes the coordinate of site α in the ith water molecule and ρ_α represents the density of site α. Compared to room-temperature results, the profiles for densities $\rho_w > 0.3$ g cm^{-3} show an almost complete loss of structure in the close vicinity of the electron center. The rise in temperature also causes a slight reduction in the distance of closest approach due to the combined effects of a higher kinetic energy of the nuclei and the obvious thermal reduction of the size of the electron polymer. Yet more noticeable are the changes that take place at low densities: For $\rho_w \leq 0.1$ g cm^{-3}, there is a considerable enhancement in the local solvent density around

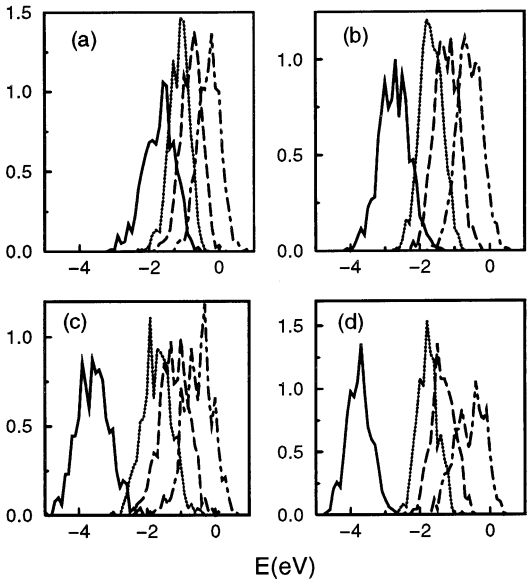

Figure 3. Normalized electron density of bound states for different densities along the $T = 645$ K isotherm. (a) $\rho_w = 0.1$ g cm^{-3}; (b) $\rho_w = 0.5$ g cm^{-3}; (c) $\rho_w = 1$ g cm^{-3}. Also shown are the results at ambient conditions (d). Solid lines correspond to ground states. Dotted, dashed, and dash−dotted lines correspond to the first, second and third excited states, respectively.

the electron centroid compared to the average bulk value. Similar density enhancements have been found in the supercritical hydration of classical ions such as Cl^-, where the pair correlation g_{Cl-O} reaches values close to 7.[23] However, for the electron case, these effects are significantly reduced due to the charge delocalization exhibited by the electron polymer, which in this density regime, is on the order of 5−6 Å. The two lowest density profiles also provide an idea of the extent of electron tunneling into the solvent: Depending on the density considered, the coordination numbers shown in Figure 2 indicate that there are typically between 1 and 2 neighboring water molecules within a distance r comparable to the gyration radius of the polymer $\sim R/2$. To acquire a pictorial idea of the two limiting electronic behaviors, the bottom panel of Figure 2 depicts typical snapshots of quasi-free (a) and localized (b) electron configurations. In the former case, one can clearly see how the delocalized electron "wets" a few nearby water molecules. We now turn to the electron density of states and the optical absorption spectra. The latter were computed within the dipolar approximation from the expression

$$I(E) \propto E(1 - e^{-\beta E})\langle \sum_{i>0,\epsilon_i<0} |\langle\psi_0|\hat{\boldsymbol{\mu}}|\psi_i\rangle|^2 \delta(\epsilon_i - \epsilon_0 - E)\rangle \quad (3)$$

where ϵ_i and $|\psi_i\rangle$ represent the ith electronic eigenstate and eigenfunction, respectively. For these computations, we first selected 800 statistically uncorrelated solvent configurations obtained along the PIMD runs, from which electron eigenvalues and eigenfunctions were computed by means of the block Lanczos procedure combined with split operator fast Fourier transform techniques described in ref 24. The electronic wave functions were represented by plane waves with 16^3 grid points. Results for the density of states are depicted in Figure 3. Similar to what is found at room temperature,[12,26] the distributions of bound states at supercritical conditions include four states: A ground s-like state and three, nondegenerate, somewhat more delocalized excited states, with p-like characteristics. Inspection of panels a−c reveals that the main effects of lowering the solvent density are reflected in a gradual shift in the position of the ground-state distribution toward higher energies, while the distributions for the first few excited states remain practically unchanged. A similar trend has also been reported in the distributions of the delocalized LUMO (identified as possible precursor states for solvated electrons) and the LUMO+1 Kohn−Sham orbitals of supercritical water in a recent ab initio molecular dynamics simulation study.[25] Note that at $\rho_w = 0.1$ g cm^{-3}, there are no major differences in the energy gaps between the four consecutive bound states. Temperature effects are much less important, and there is only a slight broadening in the distribution of ground state energies, due to larger shape fluctuations in the electron trapping cavities. The physical picture that emerges from these observations suggests that a simple particle in a fluctuating soft box model is likely to account for the reduction in the energy gaps due to the larger box length at lower densities. On the other hand, we tend to believe that the absence of any relevant feature with increasing temperature results from the partial cancellation of two terms: A reduction in the electron-water attractions—due to the significant drop in the dielectric constant of the environment—combined with a reduction in the length scale that characterizes excluded volume effects in the effective electron-water interaction due to the thermal reduction in the size of the electron. The computed ground state absorption spectra at four supercritical densities and at room temperature are shown in Figure 4. The position of the maximum at $T = 298$ K is slightly blue-shifted compared to experimental data, as noted elsewhere.[26] Similar to the density of states (Figure 3), temperature alone does not lead to significant changes in the absorption band. Hamiltonians that include many-body polarizability effects yield better estimates of the room-temperature spectra but also fail to reproduce experimental spectra in hot water.[15] At lower densities, ($\rho_w \leq 0.5$ g cm^{-3}), however, where interaction induced effects are less important, the maxima of our simulated spectra are in reasonable agreement with the experimental data at similar thermodynamic conditions (see inset of Figure 4), being 0.2−0.3 eV below the two experimental values at the lowest density for which the spectrum has been calculated (0.1 g cm^{-3}). The analysis of the spectrum at even lower densities, where all energy gaps become comparable to k_BT, requires transitions from different excited states and has not been performed here.

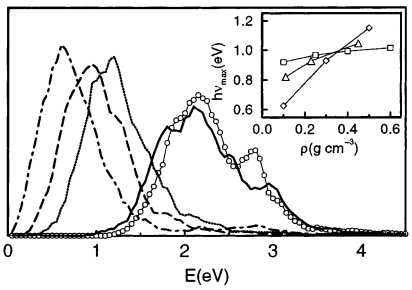

Figure 4. Ground-state absorption spectra at $T = 645$ K for different solvent densities. Thick solid line, 1.0 g cm^{-3}; solid line, 0.5 g cm^{-3}; dashed line, 0.3 g cm^{-3}; dot−dashed line, 0.1 g cm^{-3}. Also shown is the spectrum at ambient conditions (line with circles). The inset shows the density dependence of the absorption maxima in the low-density interval investigated. Diamonds, this work; squares, ref 3; triangles, ref 6b.

IV. Conclusions

The computer simulations presented here provide new insights on the microscopic nature of the electronic states and electron tunneling in supercritical aqueous environments. We find that

the transition from quasifree to localized states expressed in terms of the geometrical description of the electron takes place at a density regime where repulsions due to excluded volume effects in the electron−water pseudopotential should play a minor role in determining the electronic localization. This leads to the conclusion that the characteristics of charge density fluctuations of the different environments are in fact the key mechanisms responsible for the electronic localization in supercritical water. In our analysis, the onset of the electron localization−delocalization transition is described by qualitative changes that take place in (i) the lengthscale that characterizes the size of the isomorphic electron-polymer, which in turn represents the thermally averaged spatial extent of the electron, and (ii) the attendant variations of the solvent density fields around the electron centroid. These criteria place the transition somewhere near $\rho_w = 0.15$ g cm^{-3} at 645 K for SPC water. This value is much higher than the early experimental estimates based on features of the optical absorption spectrum ($\rho_w < 8 \times 10^{-3}$ g cm^{-3} for temperatures above the critical point).[3] In contrast, electron localization criteria based on mobility measurements at nearly critical conditions, place the transition near 0.05 g cm^{-3} at 523 K.[8] At higher temperatures, however, the transition is expected to occur at higher densities,[8,22] which, therefore, should improve the comparison with our simulations.

The optical absorption spectra for supercritical states of water extracted from our simulations reproduce the experimental values reasonably well, although the density dependence of the spectral red shift in the range 0.1 g cm^{-3} $\leq \rho_w \leq$ 0.5 g cm^{-3} is somewhat more pronounced than that experimentally measured. There are apparently no noticeable changes in the density dependence of the spectral band maximum as the localization transition is crossed. Anyhow, the overall quality of agreement is comparable to that found at room temperature, which reveals a remarkable performance of the adopted model in view of the simplicity of the interaction potentials used, the fact that we have introduced no adjustable parameters, and the wide variety of aqueous ambients examined. Additional simulation experiments are surely called for to further investigate the characteristics of the electron mobility—especially at steam-like densities—so as to establish whether there are connections between the electronic and solvent dynamics and the topology of the different microenvironments that determine the electron spectra. Finally, more elaborate descriptions for the electron−solvent pseudopotential will also deserve further investigation. In low-density polar fluids, the observed large density fluctuations are likely to be accompanied by similarly large charge fluctuations as well. The temporal characteristics of the latter are normally characterized by sufficiently short time scales that require a more rigorous quantum treatment, at least in connection to the intramolecular degrees of freedom of the bath. Even in much simpler model fluids than the SPC presented here, the incorporation of such effects is known to lead to important modifications in the delocalization−localization transition.[27]

Acknowledgment. D.L. is a member of Carrera del Investigador Científico de CONICET (Argentina). Financial support from Fundación Antorchas (Argentina) and Vitae (Brazil) is very much appreciated. M.S. also thanks the Brazilian agencies FAPESP (01/09374-3) and CNPq.

References and Notes

(1) For recent advances in technological processes involving supercritical fluids, see: *Innovations in Supercritical Fluids, Science and Technology*; Hutchenson, K. W., Foster, N. R., Eds.; ACS Symposium Series 608; American Chemical Society: Washington, DC, 1995. Kim, S.; Johnston, K. P. In *Supercritical Fluids, Chemical and Engineering Principles and Applications*; Squires, T. G., Paulatis, M. E., Eds.; ACS Symposium Series 329; American Chemical Society: Washington, DC, 1987.

(2) Tucker, S. C. *Chem. Rev.* **1999**, *99*, 391. Goodyear, G.; Tucker, S. C. *J. Chem. Phys.* **1999**, *111*, 9673. Tucker, S. C.; Maddox, M. W. *J. Phys. Chem. B* **1998**, *102*, 2437.

(3) Gaathon, A.; Czapski, G.; Jortner, J. *J. Chem. Phys.* **1972**, *58*, 2648. Jortner, J.; Gaathon, A. *Can. J. Chem.* **1977**, *55*, 1801.

(4) Michael, B. D.; Hart, E. J.; Schmidt, K. *J. Phys. Chem.* **1971**, *75*, 2798.

(5) Wu, G.; Katsumura, Y.; Muroya, Y.; Li, X.; Terada, Y. *Chem. Phys. Lett.* **2000**, 325, 351. *Radiat. Phys. Chem.* **2001**, *60*, 395.

(6) (a) Bartels, D. M.; Cline, J. A.; Jonah, C. D.; Takahashi, K. *Abstract of the American Chemical Society Meeting,* Washington, DC, Aug 2001; American Chemical Society: Washginton, DC, 2001; Part 2, pp 222−263-PHYS. (b) Cline J. A.; Jonah, C. D.; Bartels, D. M. In *The Solvated Electron in Supercritical Water: Spectra, Yields, and Reactions*, Proceedings of the 1st International Symposium in Supercritical Water-cooled Reactors, Design, and Technology, Tokyo, Nov 6−9, 2000; SCR-2000.

(7) Dimitrijevic, N. M.; Takahashi, K.; Bartels, D. M.; Jonah, C. D. *J. Phys. Chem. A* **2001**, *105*, 7236.

(8) Giraud, V.; Krebs, P. *Chem. Phys. Lett.* **1982**, *86*, 85.

(9) Krebs, P.; Heintze, M. *J. Chem. Phys.* **1982**, *76*, 5484.

(10) Using a distribution of electron traps, spectral shifts for simulated aqueous electrons have been reported in: Romero, C.; Jonah, C. D. *J. Chem. Phys.* **1989**, *90*, 1877.

(11) Laria, D.; Wu, D.; Chandler, D. *J. Chem. Phys.* **1991**, *95*, 4444.

(12) Wallqvist, A.; Thirumalai, D.; Berne, B. J. *J. Chem. Phys.* **1987**, *86*, 6404.

(13) Sprik, M.; Impey, R. W.; Klein, M. L. *J. Stat. Phys.* **1986**, *43*, 949.

(14) Schnitker, J.; Rossky, P. J. *J. Chem. Phys.* **1987**, *86*, 3471. Schwartz, B. J.; Rossky, P. J. *J. Chem. Phys.* **1994**, *101*, 6902, and references therein.

(15) Wallqvist, A.; Martyna, G.; Berne, B. J. *J. Phys. Chem.* **1988**, *92*, 1721.

(16) Wallqvist, A.; Thirumalai, D.; Berne, B. J. *J. Chem. Phys.* **1986**, *85*, 1583. Barnett, R. N.; Landman, U.; Cleveland, C. L. *Phys. Rev. Lett.* **1987**, *59*, 811.

(17) Chandler, D.; Wolynes, P. G. *J. Chem. Phys.* **1981**, *74*, 4078.

(18) Tuckerman, M. E.; Berne, B. J.; Martyna, G.; Klein, M. L. *J. Chem. Phys.* **1993**, *99*, 2796.

(19) Berendsen, H. J. C.; Postma, J. P. M.; van Gunsteren, W. F.; Hermans, J. In *Intermolecular Forces*; Pullman, B., Ed.; Reidel: Dordrecht, The Netherlands, 1981.

(20) Schnitker, J.; Rossky, P. J. *J. Chem. Phys.* **1987**, *86*, 3462.

(21) The critical temperature of the SPC model is 10% below the actual value for pure water. See: de Pablo, J. J.; Prausnitz, J. M.; Strauch, H. J.; Cummings, P. T. *J. Chem. Phys.* **1990**, *93*, 7355.

(22) Nichols, A. L., III; Chandler, D.; Singh, Y.; Richardson, D. *J. Chem. Phys.* **1984**, *81*, 5109.

(23) Re, M.; Laria, D. *J. Phys. Chem. B* **1997**, *101*, 10494.

(24) Webster, F.; Rossky, P. J.; Friesner, R. *Comput. Phys. Commun.* **1991**, *63*, 494.

(25) Boero, M.; Terakura, K.; Ikeshoji, T.; Leiw, C. C.; Parrinello, M. *J. Chem. Phys.* **2001**, *115*, 2219.

(26) Schnitker, J.; Motakabbir, K.; Rossky, P. J.; Friesner, R. *Phys. Rev. Lett.* **1988**, *60*, 456.

(27) Nichols, A. L., III; Chandler, D. *J. Chem. Phys.* **1985**, *84*, 398.